Interaction between local hydrodynamics and algal community in epilithic biofilm

Myriam Graba, Sabine Sauvage, Frédéric Moulin, Gemma Urrea-Clos, Sergi Sabater, Jose-Miguel Sanchez-Perez

Interaction between local hydrodynamics and algal community in epilithic biofilm

Myriam Graba [a,b,c,*,1], *Sabine Sauvage* [a,b], *Frédéric Y. Moulin* [d,e], *Gemma Urrea* [f], *Sergi Sabater* [f,g], *José Miguel Sanchez-Pérez* [a,b]

[a] *Université de Toulouse, INP, UPS, EcoLab (Laboratoire d'Ecologie Fonctionnelle et Environnement), Avenue de l'Agrobiopôle, 31326 Castanet Tolosan, France*

[b] *CNRS, EcoLab, 31326 Castanet Tolosan, France*

[c] *Université Abderrahmane Mira, Route de Tharga Ouzemour, 06000 Bejaia, Algeria*

[d] *Université de Toulouse, INPT, ENSEEIHT, UPS, IMFT (Institut de Mécanique des Fluides de Toulouse), F-31400 Toulouse, France*

[e] *CNRS, IMFT, F-31400 Toulouse, France*

[f] *Institute of Aquatic Ecology, Faculty of Sciences, University of Girona, Campus Montilivi, 17071 Girona, Spain*

[g] *Catalan Institute for Water Research, H_2O building, Scientific and Technological Park of the University of Girona, Emili Grahit 101, 17003 Girona, Spain*

Keywords:
Epilithic biofilm
Experimental flume flow
Friction velocity
Biomass dynamics
Turbulent boundary layer
Algal composition

A B S T R A C T

Interactions between epilithic biofilm and local hydrodynamics were investigated in an experimental flume. Epilithic biofilm from a natural river was grown over a 41-day period in three sections with different flow velocities (0.10, 0.25 and 0.40 m s^{-1} noted LV, IV and HV respectively). Friction velocities u_* and boundary layer parameters were inferred from PIV measurement in the three sections and related to the biofilm structure. The results show that there were no significant differences in Dry Mass and Ash-Free Dry Mass (g m^{-2}) at the end of experiment, but velocity is a selective factor in algal composition and the biofilms' morphology differed according to differences in water velocity. A hierarchical agglomerative cluster analysis (Bray–Curtis distances) and an Indicator Species Analysis (*IndVal*) showed that the indicator taxa were *Fragilaria capucina* var. *mesolepta* in the low-velocity (u_* = 0.010–0.012 m s^{-1}), *Navicula atomus*, *Navicula capitatoradiata* and *Nitzschia frustulum* in the intermediate-velocity (u_* = 0.023–0.030 m s^{-1}) and *Amphora pediculus*, *Cymbella proxima*, *Fragilaria capucina* var. *vaucheriae* and *Surirella angusta* in the high-velocity (u_* = 0.033–0.050 m s^{-1}) sections. A sloughing test was performed on 40-day-old biofilms in order to study the resistance of epilithic biofilms to higher hydrodynamic regimes. The results showed an inverse relationship between the proportion of detached biomass and the average value of friction velocity during growth. Therefore, water velocity during epilithic biofilm growth conditioned the structure and algal composition of biofilm, as well as its response (ability to resist) to higher shear stresses. This result should be considered in modelling epilithic biofilm dynamics in streams subject to a variable hydrodynamics regime.

* *Corresponding author*. Permanent address: Département d'hydraulique, Université Abderrahmane Mira, Route de Tharga Ouzemour, 06000 Bejaia, Algeria. Tel.: +213 0 7 70 51 92 38; fax: +213 0 34 21 51 05.
E-mail address: mgraba@yahoo.fr (M. Graba).
[1] Present address: ENSAT/EcoLab, Avenue de l'Agrobiopôle, 31326 Castanet Tolosan, France. Tel.: +33 0 6 62 35 38 71; fax: +33 0 5 34 32 39 55.

Notations

AFDM	Ash-Free Dry Mass (g m^{-2})
DM	Dry Mass (g m^{-2})
H	Flow height (m)
k_s	Nikuradse's equivalent sand roughness (m)
k^+	Roughness Reynolds number (= $u_* k_s/\nu$)
Q	Flow discharge (m^3 s^{-1})
SE	Standard error in measured values (g m^{-2})
u^*	Friction velocity (m s^{-1})
ν	Water kinetic viscosity (10^{-6} m^2 s^{-1})

1. Introduction

"Epilithic biofilm" that grows on gravel, cobbles, and rocks in river beds, is a collective term for a complex microorganism community and includes algae, bacteria, and microfauna, with algae usually the dominant component. This community is the source of most primary production (Minshall, 1978; Lock et al., 1984), and constitutes a food source for a number of invertebrates and fish (Fuller et al., 1986; Mayer and Likens, 1987; Winterbourn, 1990). It plays a major role in the metabolic conversion and partial removal of biodegradable material in rivers and streams (McIntire, 1973; Saravia et al., 1998; Hondzo and Wang, 2002), and serves as a functional indicator of river health (Wehr and Sheath, 2003; Cardinale, 2011). However, it still one of the least-studied communities despite the significant increase in the examination of aquatic microbial communities in recent years (Stoodley et al., 2000; Battin et al., 2003; Besemer et al., 2007, 2009a, 2009b).

Hydrodynamics is one of the most important environmental factors (nutrient, light, temperature etc.) driving stream biofilm dynamics and structure and is generally considered the major agent of physical forcing on the biofilm (Reiter, 1986; Power and Stewart, 1987; Biggs et al., 2005). Indeed, metabolic rates for the biofilm are controlled by the thickness of the diffusive boundary layer that develops along filaments driving the transfer of metabolites to and from cells, and they are then related to the flow water velocity (Whitford and Schumacher, 1961; Lock and John, 1979; Riber et al., 1987). Besides, as water velocity increases, the drag forces and skin friction exerted on the community also increase, and this affects their attachment ability (Biggs and Hickey, 1994).

The effect of water velocity on epilithic biofilms biomass has been analysed in a number of studies, both by observations in natural streams (e.g. Biggs and Hickey, 1994; Uehlinger et al., 1996, 2003; Boulêtreau et al., 2006, 2008, 2010) as well as in flumes (e.g. Horner and Welch, 1981; Ghosh and Gaur, 1998; Hondzo and Wang, 2002; Cardinale, 2011). However, only local flow conditions are ultimately relevant for describing the forcing at biofilm scale, and are generally not easily inferred from mean bulk velocities, except in the case of hydraulically smooth turbulent boundary layers where only the fluid viscosity ν (Nezu and Nakagawa, 1993) and the metabolites diffusivities need to be known. For rough turbulent boundary layers, a better description of the local flow conditions are inferred by a log law description (see Labiod et al., 2007; Graba et al., 2010) that requires knowledge of the roughness length (or equivalently Nikuradse's equivalent sand roughness k_s) and reads :

$$\frac{U(z)}{u^*} = \frac{1}{\kappa}\log\left(\frac{z-d}{k_s}\right) + 8.5 \quad (1)$$

Or from the exponential profile of Nezu and Nakagawa (1993):

$$\frac{U(z)}{u^*} = D_u \exp\left(-C_k \frac{z}{H-d}\right) \quad (2)$$

where $U(z)$ is the mean (above the roughness sublayer) or double-average longitudinal velocity (inside the roughness sublayer), u_* is the friction velocity, k_s the Nikuradse's equivalent sand roughness, d the displacement height, κ the Karman constant ($\kappa = 0.41$), H the flow height and C_k and D_u are empirical constants ($C_k = 1$ and $D_u = 2.3$).

Observations on the interaction between water flow and biofilms (Reiter, 1989a, 1989b; Nikora et al., 1997, 1998; Labiod et al., 2007) have shown that friction velocity u_* (which measures the drag of the flow at the bottom layer) could increase with the growth of epilithic biofilm, leading to the conclusion that stream biofilm increased bed roughness. However, Biggs and Hickey (1994), Moulin et al. (2008) and Graba et al. (2010) have found that stream biofilm decreased the drag forces and the roughness. As explained in Moulin et al. (2008) and Graba et al. (2010), these apparently contradictory results are essentially due to a gradual transition from a completely nude bed to a biofilm-covered bed, an increase or decrease of the roughness length being observed depending on the value of the roughness length for the initial nude bed compared to a typical value for a biofilm-covered bed. Yet, beyond their apparent contradictions, these studies provide an idea of the complex interaction between local hydrodynamics and the successional stage (age, thickness and composition of the community) and physiognomy of the algal biofilm community (Reiter, 1989b).

Tools such as the hydraulic habitat preference curves (Jowett et al., 1991) have been used to predict the effects of flow regulation on stream habitats (Davis and Barmuta, 1989; Young, 1992). However, there is still a poor knowledge on the relationship between the near-substratum hydrodynamics and the structure and species composition of epilithic algal assemblages. It is generally admitted that Rhodophytes prefer current velocities exceeding 0.030 m s^{-1} (Seath and Hambrook, 1988), and that some species (*Gomphonema parvulum* and *Gomphonema lanceolatum*) prefer pools as the main habitats (Ghosh and Gaur, 1998). It is also known that while

some species (*Cladophora*, *Lemanea*) were more abundant in turbulent flow habitats (Tornés and Sabater, 2010), others (*Achnanthidium* and *Nitzshia*) dominate habitats that had experienced recent disturbances (Cardinale, 2011).

We can also refer to the experimental results of Battin et al. (2003) and Besemer et al. (2007, 2009a, 2009b) on stream microbial biofilms developed in contrasted flow conditions. These results suggest a shift from a predominantly physical control including hydrodynamics to coupled biophysical controls driven by biofilm communities, which, as "ecosystem engineers," modulate their microenvironment to create similar architectures and flow conditions and thereby reduce the physical effect of flow on bacterial community succession in stream biofilms. The last works of Singer et al. (2010) show that this biophysical mechanisms through which physical heterogeneity induces changes of resource use and carbon fluxes in streams. These findings highlight the importance of fine-scale streambed heterogeneity for microbial biodiversity and ecosystem functioning in streams, where homogenization and loss of habitats increasingly reduce biodiversity.

Thus, near-bed flow parameters should be considered instead of vertically integrated descriptors such as the mean bulk velocity that, alone, will not give any information on what is happening near the biofilm. To some extent, this use of mean bulk velocities partially explains the poor knowledge about the dynamics, structure and species composition of benthic algal assemblages. Also, it is important to have more knowledge of what is happening in the near-bed flow for the improvement of biomass dynamics models for epilithic biofilms (e.g., McIntire, 1973; Horner and Welch, 1981; Horner et al., 1983; Momo, 1995; Uehlinger et al., 1996; Saravia et al., 1998; Asaeda and Hong Son, 2000, 2001; Flipo et al., 2004; Boulêtreau et al., 2006, 2008) that almost use global descriptors of the hydrodynamics such as integrated flow discharge or velocity.

This study was conducted with two main objectives: i) to determine the specific requirements of various algal species with the near-substratum hydrodynamic regime in flows representative of the in situ conditions (growth on large substrates and hydraulically rough turbulent boundary layers), and ii) to test the detachment resistance of algal assemblages to drag and shear stress caused by sudden increases in water velocities.

2. Materials and methods

An experiment was performed in an indoor laboratory flume situated at the Institute of Fluid Mechanics (Toulouse, France). Water flow can be partially re-circulated with the Garonne River in order to avoid nutrient limitation while controlling the hydrodynamical conditions (Fig. 1). The experimental flume (Godillot et al., 2001; Labiod et al., 2007; Graba et al., 2010) was built with Plexiglas sides (10 mm thick) and a PVC base (20 mm thick). It was 1 1m long, 0.5 m wide, 0.2 m deep and with a 10^{-3} slope. The flume was adapted for this study to have three different flow conditions by modifying its width and depth (Fig. 2). Three bulk velocities (0.10, 0.27 and 0.40 m s^{-1} in the corresponding LV or low-velocity, IV or intermediate-velocity and HV or high-velocity sections) were generated. The flume had a first pump that continuously supplied water from the river to the outlet reservoir (3300 L) and a second submerged pump that supplied water to the inlet reservoir (1500 L) with a fixed volumic discharge Q = 6 L/s. The water flowed between the two reservoirs through the experimental flume by gravity. The suspended matter from the Garonne River water was eliminated by two centrifugal separators, and the water was then filtered three times through filters with 90, 10, and 1 μm pores. Illumination was supplied by three sets of 1.6 m-long horticultural fluorescent tubes, in a 12-h day: 12-h night photoperiod. A cooling system allowed water temperature to be maintained at between 17 and 23 °C. The bottom of the flume was completely covered by artificial hemispherical cobbles (see Fig. 2) of sand-blasted polyurethane resin, used in other published works (Boulêtreau et al., 2010; Graba et al., 2010). The artificial cobbles were 37 mm in diameter and H = 20 mm in height. This shape and texture provided good conditions for epilithic biofilm adhesion and growth (Nielsen et al., 1984). The cobbles were not fixed to the flume bottom for ease of sampling. In addition, 4 patches of 12 or 16 cobbles in each of the three sections were attached to plastic plates in order to be removed and placed in the sloughing test flume at the end of the growth experiment.

The experiment was performed in three stages. The first one lasted for three weeks and consisted of biofilm seeding. At this stage, the water was re-circulated in the flume, renewed

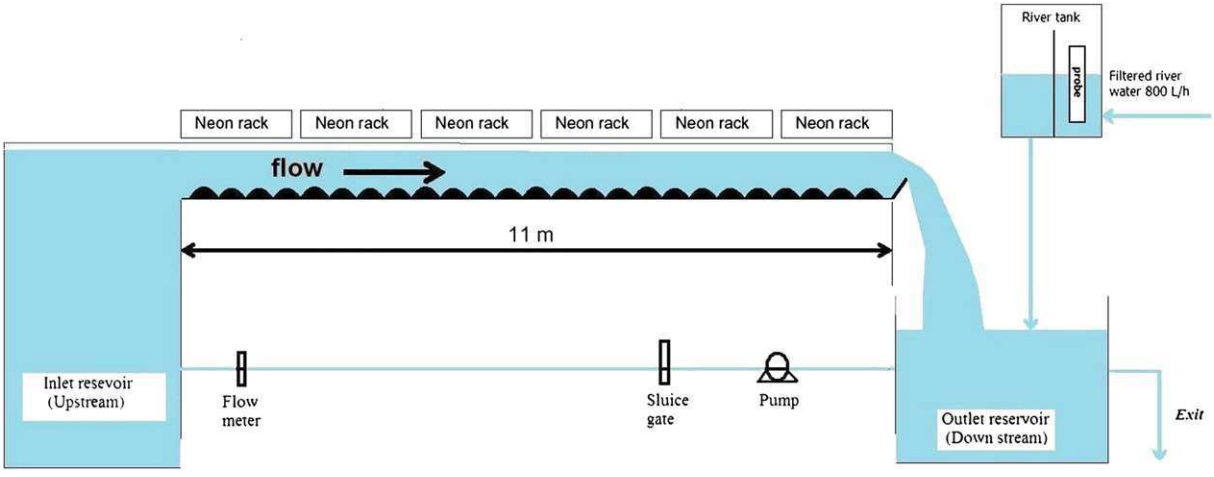

Fig. 1 — Longitudinal view of the experimental flume.

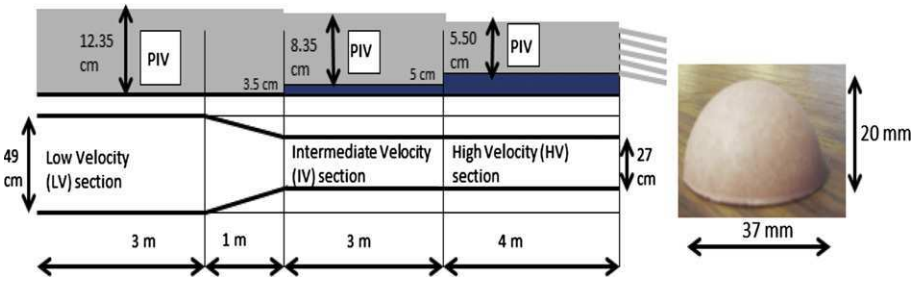

Fig. 2 — Sketch of the principal laboratory flume, with locations of the PIV measurement access windows and the dimensions of the artificial cobbles.

weekly, and just after renewal seeded again with a biofilm suspension. The biofilm suspension was produced by scraping the upper surface of 15 randomly selected pebbles in nearby streams with a toothbrush. The biofilm suspension was homogenised (tissue homogeniser), and the macro fauna removed to minimise the effect of grazers. After the seeding (inoculum) stage, the flume changed to open water circulation to allow the free growth of epilithic biofilm. During this stage, hydrodynamic and biological measurements were performed weekly. Furthermore, upper view images of the artificial cobbles were taken daily through a Plexiglas window in the three sections (HV, IV and LV) using a digital camera (Nikon, 2000 × 1312 pixel resolution). The last stage of the experiment (after 41 days) consisted of a resistance test to sloughing conducted in a separate 20 m-long by 21 cm-wide by 40 cm-deep laboratory flume, whose last 12 m were covered with artificial cobbles in order to generate the same turbulent boundary layer structure as in the growth flume, but with different values of friction velocity u_*. In this stage, samples of the three different kinds of cultivated biofilms were placed 6 m downstream from the start of the sloughing test flume in a 10 cm space that was left free for positioning plastic plates with 12–16 sampled substrates from each of the three different sections (HV, IV and LV). The samples were then exposed to increasing flow velocities by a discharge ramp of 0.005 $m^3\ s^{-1}$ every 2 min to shift friction velocity from 0.0 to 0.064 $m\ s^{-1}$.

2.1. Biological sampling and measurements

2.1.1. Epilithic biomass

Biofilm biomass was sampled every week after the seeding phase. Four cobbles were selected randomly in each of the three HV, IV and LV sections. The sampled cobbles on each sampling occasion were kept in sterile vials at 4 °C. The cobble rows closest to the walls were not sampled to avoid edge effects. Every cobble sampled was replaced with a new pink-coloured one to avoid re-sampling. The sampled cobbles were dried (80 °C, overnight) to obtain the dry weight. The scraped dry matter was again weighed after combustion (500 °C, overnight) to determine ash free dry mass (AFDM) weight. The AFDM was expressed in $g\ m^{-2}$ after considering the total surfaces of the 4 hemispherical cobbles. The AFDM in the sloughing test flume was also determined in 4 cobbles before and another four after the increasing discharge ramp.

2.1.2. Algal composition

Three samples to analyse the diatom community composition were collected in the experimental flume after 37 days. The samples were collected at the entrance, at the middle and at the final part of each of the three LV, IV and HV sections. Samples from the LV section were named as A1, A2 and A3, those in the IV section as B1, B2 and B3, and those in the HV section as C1, C2 and C3. Biofilm was scraped off with a sterile toothbrush, suspended in filtered (0.2 μm) water (50 mL glass vials), and preserved with glutaraldehyde (1% final concentration) in cool, dark conditions until examination at 1000X. The species identification was completed at the lowest taxonomic level. Square root transformation was used in order to down-weight high values of the relative abundance (%) of species. We used hierarchical agglomerative cluster analysis by means of the complete linkage (furthest neighbour) in order to classify the samples based on their similarity, using Bray–Curtis distances. In order to identify species discriminating among the cluster groups, an Indicator Species Analysis (*IndVal*) (Dufrène and Legendre, 1997) was performed with untransformed abundance data. The analyses were performed using PRIMER-6 (Clarke and Gorley, 2005) and PC–ORD (McCune and Mefford, 1999).

2.2. Hydrodynamic measurements

During the biofilm growth, Particle Image Velocimetry (PIV) measurements were performed in two vertical planes in the middle of the tank (one longitudinally aligned plane just over the top of the hemispheres, and another one 1 cm apart) in the three different sections. The laser sheet was created by a pulsed Nd : YAG laser system (532 nm, 2 × 30 mJ/pulse), and the images were captured by a Sensicam camera (1280 × 1024 pixels, 12 bits) with resolutions from 75 to 150 pixels/cm. PIV particles were injected upstream the measurement region to improve the quality of images. For each vertical plane, 1000 independent instantaneous velocity fields, yielding the longitudinal and vertical components u and w, were calculated using spatial correlation techniques with peak-locking reduction algorithms developed by Fincham and Spedding (1997), and Fincham and Delerce (2000). The smallest scale resolved was around 1.5 mm, i.e. about 10-30η, where $\eta = (\nu^3 H/34\ u^3)$ is an estimated Kolmogorov scale given by Coceal et al. (2006) for rough turbulent boundary layers. The spatial accuracy was then high enough to estimate correctly both

mean values and fluctuations of u and w, as defined in the Reynolds decomposition $u = \overline{u} + u'$ and $w = \overline{w} + w'$. Each vertical plane yields 120 vertical profiles along around 8 cm, i.e., two hemisphere diameters in the streamwise direction.

Following the methodology of Nikora et al. (2002, 2007a, 2007b), double-averaged quantities, i.e. quantities averaged in the two horizontal directions (noted with brackets$< >$) were estimated from PIV measurements in the two vertical planes by spatial averaging along the streamwise direction and between the two vertical planes. As shown by Castro et al. (2006), such double-averaged quantities extend the validity range of the log law towards the top of the roughness, deep inside the roughness sublayer, leading to more robust estimations of the boundary layer parameters u_*, k_s and d. The 1000 independent measurements of u and w yield to an estimation of $\langle \overline{u} \rangle$ and$< \overline{u'w'} >$ with time convergence relative errors below 5% and 15%, respectively (using convergence error estimates of Bendat and Piersol (1971) for confidence intervals of 95%). To fit the data with the log-law equation (1), we followed Castro et al. (2006) and inferred the friction velocity u_* from vertical profiles of the turbulent shear stress $< \overline{u'w'} >$: we took the square root of the averaged value of the turbulent shear stress in both the roughness and inertial sublayers. For nude cobbles before the inoculum, it corresponded to the region between the top of the hemispheres at $z = H$ and the top of the inertial sublayer, taken as $z = 0.1(D\text{-}H)$ where D is the water depth in order to remain far below the defect law region. For biofilm-covered cobbles, algal filaments moved in the camera field, so that the top for the roughness could not be clearly identified like for nude cobbles. Therefore, we used the maximal height reached by the filaments, noted z_{top}, as the lower limit of the fitting range of the log-law equation (1). Naturally, with biofilm accrual, this lower limit gradually raised up from 2 cm for the nude cobbles to 3.5 cm for the 28 days old biofilm in the low velocity section. The upper limit of the fitting range was chosen equal to the top of the inertial sublayer at $z = z_{top}+0.1(D\text{-}z_{top})$. Further details on this method and on PIV measurements are presented in Moulin et al. (2008) and Graba et al. (2010). Relative errors on $< \overline{u'w'} >$ below 15% yield errors on friction velocity u_* lower than 7.5%. With fitting ranges defined above, relative errors on k_s and d induced by errors on $\langle \overline{u} \rangle$ and$< \overline{u'w'} >$ were found to be lower than 10%.

The roughness Reynolds number k^+ ($=u_* k_s/\nu$, where ν is water kinetic viscosity), a descriptor of the hydraulic roughness of the flow was also calculated. This number depends on the hydraulics and turbulent conditions in the near bed region (turbulent energy) but also on the dimensions and the shape of the roughness in this region (that drives the shape of the mean velocity profile). So the change of the values of this term gives an idea of the changes induced by the growth of the epilithic biofilm on the turbulent conditions and the flow regime in the near bed region. More specifically, for vegetal canopies, vertical exchanges of matter between the canopy and the flow above can be expressed using exchange velocity or equivalently, power functions of k_s, as discussed in Graba et al. (2010).

In the sloughing test flume, PIV measurements were also performed at different values of the volumic discharge Q, and the boundary layer parameters (friction velocity u_*, Nikuradse's equivalent sand roughness k_s, and The roughness Reynolds number k^+) were then inferred at the same way than in the main channel. As expected for rough turbulent boundary layers over rigid bottom, log law parameters d and k_s were independent of Q, with $d \approx 1.54 \pm 0.02$ cm and $k_s \approx 1.03 \pm 0.07$ cm for all values of Q. Measured friction velocities u_* were found to be linearly dependent of Q, with values of $u^* = 1.0$, 1.8, 3.0, 4.1, 5.1 and 6.4 cm s^{-1} for respectively Q = 5, 10, 15, 20, 25 and 30 Ls^{-1}.

3. Results and discussions

3.1. *Biofilm biomass*

The temporal evolution of DM and AFDM (g m^{-2}) in the three flow sections (Fig. 3 and Fig. 4) reveals that flow velocities have a significant influence on the values of DM at days 9 (ANOVA, $P < 0.001$), 15 (ANOVA, $P < 0.001$) and 23 (ANOVA, $P < 0.05$). Later (on days 29 and 35) these differences became less significant ($0.05 < P < 0.2$). AFDM was less sensitive to water velocity patterns. The influence of flow velocity on AFDM was significant only up to day 15 (ANOVA, $P < 0.05$) and became insignificant at days 23, 29 and 35 ($0.05 < P < 0.2$).

These results show that the biofilm colonisation was significantly delayed by the highest flow velocity until the third week after inoculum, but the values reached at the end of the experiment approached a mean of 93.95 ± 15.74 (g m^{-2}, DM) and 23.10 ± 4.03 (g m^{-2}, AFDM) for the three sections. This can be explained by the conflicting effects of current regime and turbulence intensities. In fact, in the initial colonisation phase the highest drag forces and friction velocities slowed down the deposit and attachment of microbial and algal cells, resulting in a more significant colonisation in the low flow regime than in the higher ones. From the third week of the experiment, the highest diffusion and exchange in the intermediate and high-flow region accelerated the productivity of the attached cells and counterbalanced the delay registered during the colonisation phase.

3.2. *Biofilm patterns and algal composition*

Colonisation patterns during the first week were regular in the LV section, i.e. exhibiting the same spatial distribution for

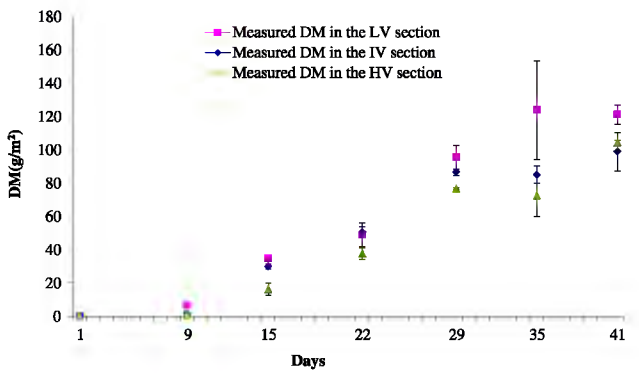

Fig. 3 – Evolution of the DM ± SE (g m^{-2}) in the three flow sections (LV, IV and HV) at different days after inoculum.

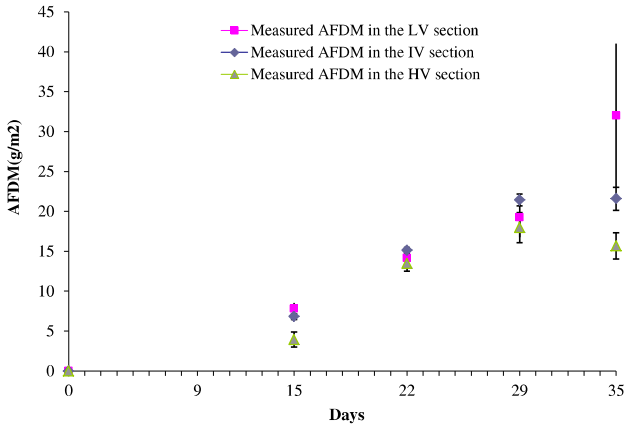

Fig. 4 — Evolution of the AFDM ± SE (g m^{-2}) in the three flow sections (LV, IV and HV) at different days after inoculum.

every hemisphere, while patchier and more randomly distributed in the IV and HV sections. It took the shape of an initial patch located at the front stagnation point of the flow in the three sections, and an annular distribution in the recirculation zone at the rear of the hemispheres in the LV section. Then, the biofilm spread over the whole hemisphere, initially along an approximatively horizontal line crossing the front stagnation point (see Fig. 5e). This is in agreement with flow conditions near the hemispheres that are exactly the same initially, both in terms of mean velocity quantities and turbulent quantities, because of the periodic distribution of hemispheres, supporting colonization success in particular regions (stagnation points or lines associated with low shear stress on the hemisphere surface). Moreover, both top view images and biomass measurements at day 8 show that the biomass accrual during the colonization decreases with the value of the friction velocity u^*, in accordance with what was observed by Stoodley et al. (2000) for bacterial biofilms.

Later, after the colonization phase, the general pattern observed was that biofilms developed under lower velocities were thicker and had larger surface sinuosity and higher areal densities than their counterparts exposed to higher velocities. This result has been already observed in other experiments with microbial biofilms or stream (Battin et al., 2003; Tornés and Sabater, 2010). The biofilm at the end of experiment exhibited rather different physiognomies: a thick mat, with long and very thick filaments extending over at least two hemisphere diameters (i.e. up to 10 cm, see Fig. 5d) in the LV section; more compact biofilms in the IV and HV sections, with ca. 3 cm-long thick filaments in the IV section, and 3 cm-long but very thin filaments in the HV section (Fig. 5e).

On a total of 72 diatom species counted, the dominant species was the centric diatom *Melosira moniliformis (O.F.Muller) Agardh* in all samples (21.53% in A1, 22.43% in A2, 26.84% in B1, 14.32 in B2, 18.59% in B3, 19.25% in C1, 26.95% in C2 and 21.73% in C3) except in sample A3 where *Fragilaria capucina var. mesolepta (Rabh) Rabenhorst* was dominant (24.06%). This dominant centric diatom species has a structure associated with secretions on the valve surface which bind the cells together in linear colonies (Wehr and Sheath, 2003; Leflaive et al., 2008), and give a more or less filamentous aspect to the biofilms, depending on the drag forces caused by the hydrodynamics in the near-bed layer (Cardinale, 2011) .This dependence explain the difference in the structure and the longer of the filaments developed in the three sections (LV, IV and HV).

The number of species between sections was similar: 40 in the LV section, 44 in the IV section and 39 in the HV section. A cluster analysis including all the samples grouped them by water velocity (Fig. 6). According to the *IndVal* (Table 1), *Fragilaria capucina* var. *mesolepta* was the indicator taxa in the low velocity group, *Navicula atomus*, *Navicula capitatoradiata* and *Nitzschia frustulum* were the indicator taxa in the mid velocity group and *Amphora pediculus*, *Cymbella proxima*, *Fragilaria capucina* var. *vaucheriae* and *Surirella angusta* were the indicator taxa in the high velocity group. Species in the low-velocity

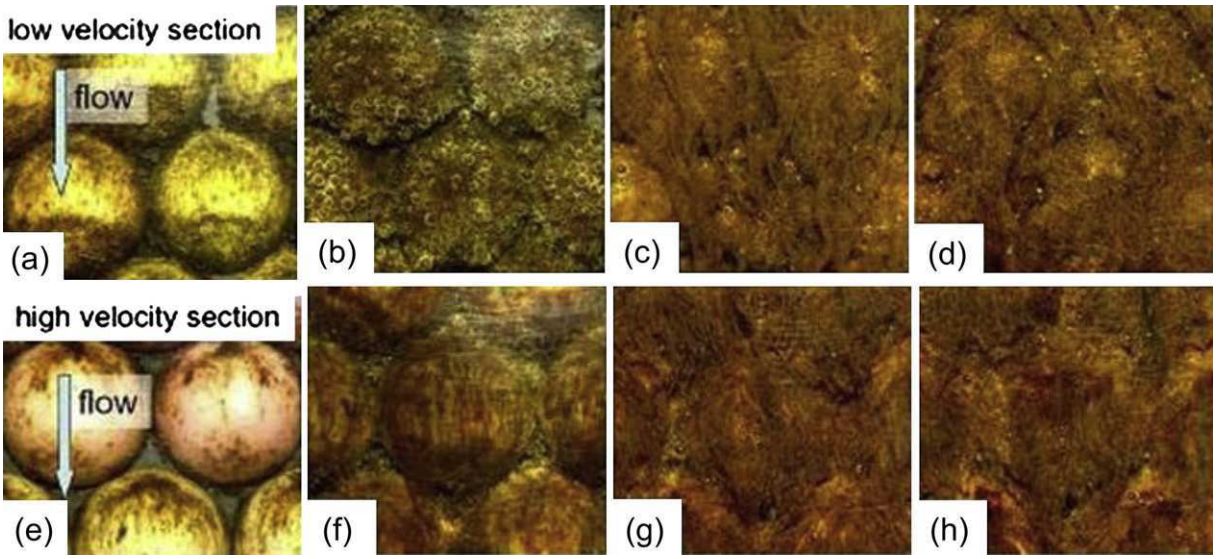

Fig. 5 — Top views of the epilithic biofilm evolution in the LV and HV sections at 8 (a, e), 14 (b, f), 21 (c, g) and 28 (d, h) days after inoculum (flow from top).

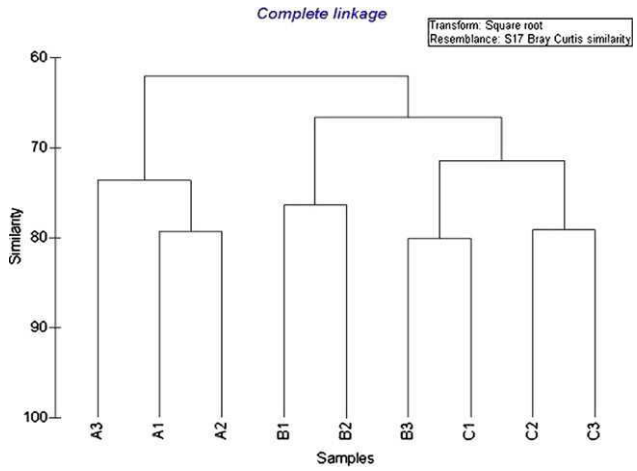

Fig. 6 — Hierarchical cluster analysis of algal data based on the furthest neighbour method and Bray–Curtis distance. The axis indicates the % of remaining information between groups.

group are multi-cellular growth forms which have been described at low water velocities (Blum, 1957; Whitford and Shumacher, 1961; Tornés and Sabater, 2010). These species are replaced by smaller unicellular free adnate or prostrate forms (*Navicula, Nitzschia, Amphora*) in higher water velocities (Martínez De Fabricius and Sabater, 2003) and gave a more compact aspect for the biofilms in the IV and HV sections. Drag forces mostly affect larger algae because small cells may lie within the boundary layer where frictional forces between water and substratum slow the flow (Silvester and Sleigh, 1985). Also, *Navicula* and *Nitzschia* maintain contact with various surfaces and glide through the micro-habitat by means of a slit in the wall of the valves called a raph, while *cymbella* attaches itself using gelatinous pads or stalks and *Amphora* is known to have an extreme asymmetric shape that makes it attach firmly to substrata. Those characteristics make the last species more resistant to wave scour or other disturbance (Wehr and Sheath, 2003).

Other species (*Achnanthidium saprophila (Kobayasi et Mayama) Round & Bukhtiyarova, Navicula reichardtiana Lange-Bertalot, Nitzschia fonticola Grunow in Cleve et Möller* and *Sellaphora seminulum (Grunow) D.G. Mann*) were also somewhat

Table 1 — Indicator species of each cluster group. S = Specificity measure; F = Fidelity measure and *IndVal* = Indicator value.

	$P < 0.05$	A (A1, A2, A3)			B (B1, B2)			C (B3, C1, C2, C3)		
		S	*F*	*IndVal*	*S*	*F*	*IndVal*	*S*	*F*	*IndVal*
Fragilaria capucina var. mesolepta (Rab) Rabenhorst	0.04	51	100	51	29	100	29	20	100	20
Navicula atomus (Kutz.) Grunow	0.05	0	0	0	69	100	69	31	75	23
Navicula capitatoradiata Germain	0.02	30	100	30	42	100	42	28	100	28
Nitzschia frustulum (Kut.) Grunow	0.01	18	67	12	50	100	50	32	100	32
Amphora pediculus (Kut.) Grunow	0.02	36	67	24	0	0	0	64	100	64
Cymbella proxima Reimer	0.01	0	0	0	0	0	0	100	100	100
Fragilaria capucina var. vaucheriae (Kut.) Lange-Bertalot	0.05	27	67	18	25	100	25	48	100	48
Surirella angusta Kutzing	0.04	30	33	10	0	0	0	70	100	70

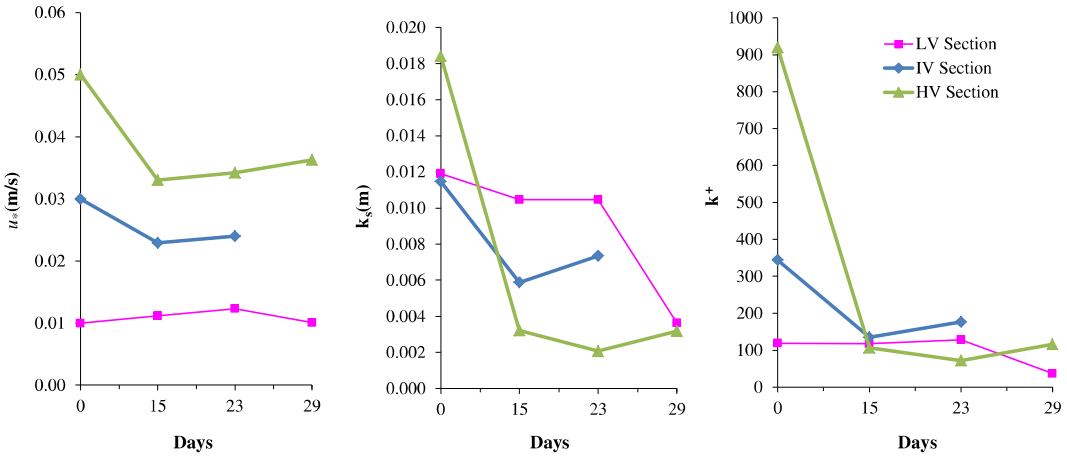

Fig. 7 — Variation of the friction velocity u_* and roughness Reynolds number k^+ during epilithic biofilm colonisation and growth.

abundant (>5%) but did not show preferences with regard to the three current regimes.

3.3. *Evolution of hydrodynamics and near-bed parameters of the flume*

During epilithic biofilm growth in the relatively deep water conditions (LV section), Nikuradse's equivalent sand roughness k_s values remain initially close to the value found for artificial cobbles without biofilm, i.e. 0.01 m and no significant modifications in friction velocity u_* and roughness Reynolds number k^+ were observed (Fig. 7) as long as the biofilm structure remained relatively compact. However, a very clear drop in k_s (towards values close to 0.0035 m) was measured as soon as long and thick filaments became dominant in the last two weeks of the experiment, and exceeded the initial spatial wavelength prescribed by the artificial cobbles (see Fig. 7b).

In contrast, for biofilm growing in the IV and HV section on macrorugosities in shallow water conditions (i.e. when the vertical dimension of the roughness is not small in

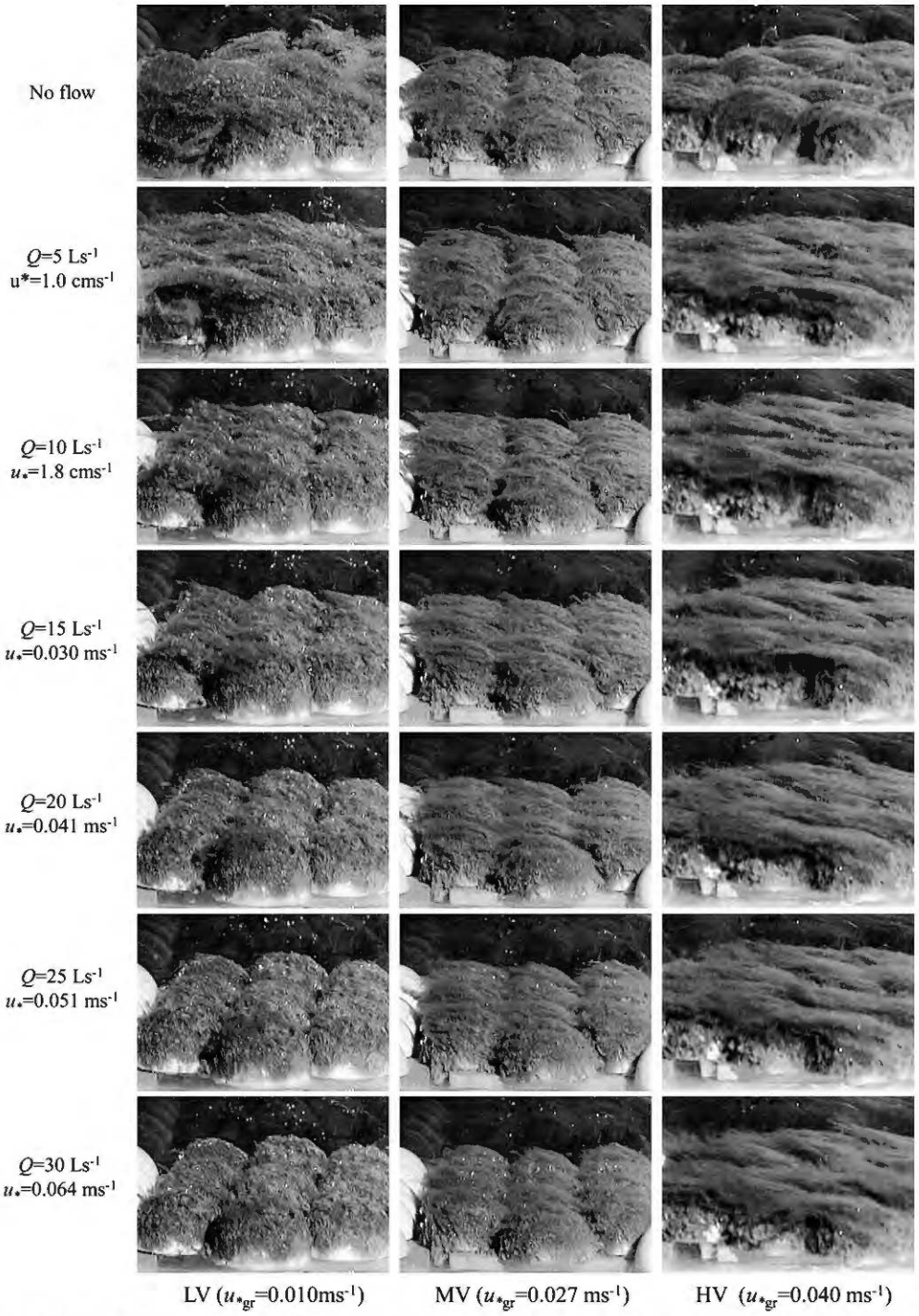

Fig. 8 – Side views of the epilithic biofilm in the LV (left), MV (middle) and HV (right) sections during sloughing test and for increasing sloughing friction velocity.

Table 2 – Measurements of biomass (DM) in the sloughing test flume with u_* up to 0.064 ms^{-1}).

Flume section	u^*_{gr}, average values of friction velocity during biofilm growth (ms^{-1})	DM ± SE before sloughing (gm^{-2})	DM ± SE after sloughing (gm^{-2})	Detached proportion
LV	0.010	121.39 ± 2.94	57.9 ± 18.56	52%
IV	0.025	99.11 ± 11.50	70.7 ± 10.85	29%
HV	0.040	104.49 ± 1.25	93.5 ± 3.27	11%

comparison with water depth), the evolution is very different. Very confined flows are generated initially ($\Delta/h = 4$ and 3), and a very quick decrease in the Nikuradse's equivalent sand roughness k_s and friction velocity u_* is observed (Fig. 7) at the beginning of experiment when the biofilm matter covered firstly the troughs between the cobbles spaces (see Fig. 5e) and brought about a change in the roughness topography, leading to a less rough boundary associated with less strong drag, so a decrease in friction velocity u_* and the turbulent roughness k^+ were observed (see Fig. 7).

As discussed in Moulin et al. (2008), competing contributions from the wake and skin frictions behind cobbles and along algal filaments necessarily drive a complex evolution of the roughness length since this quantity integrates all the processes occurring in the canopy (see Nikora et al., 2007a, b). The drop of k_s in deep flows is observed when filaments become longer than the initial horizontal scale prescribed by the substrates, the biofilm structure then controlling most of the friction. Indeed, the values of k_s found at the end of the growth experiment in the present study, equal to 0.318×10^{-3} m for the HV section and 0.360×10^{-3} m for the LV section at day 28, compare very well with the values found by Labiod et al. (2007) for same age biofilms grown on smaller substrates (values found range between 0.468 and 0.800×10^{-3} m for 26-day-old biofilm). The main difference between the two studies comes from the difference in the initial value of k_s that depends only on the substrate length scale (rods or marbles in Labiod et al. (2007) and around 2×10^{-3} m high hemispheres in our study). These flow measurements confirm an evolution of k_s that simply expresses a transition from a bed covered with nude substrates towards a bed covered completely with a matt of biofilm.

The evolution of the near bed turbulence (evaluated by the roughness Reynolds number k^+) as we can see in Fig. 7, agree with the result of Besemer et al. (2007, 2009a, 2009b) and Tornés and Sabater (2010) that the algal mats as the bacterial community modify the local architectural conditions in a way to slow down the near-substratum velocities, and thereby lessening the current effects on algal and bacterial detachment.

3.4. *Sloughing test*

During the sloughing test, increasing friction velocities were exerted on the sampled cobbles by increasing the flume flow discharge Q. For Q ranging from 0.005 m^3 s^{-1} to 0.030 m^3 s^{-1}, PIV measurements yield values of friction velocity that range between 0.010 and 0.064 m s^{-1}.

Filming during the sloughing test (see Fig. 8) shows that the detachment of filaments begins after the friction velocity value exerted in the sloughing flume exceeds the time-averaged value exerted during the growth experiment in the section being considered (noted u^*_{gr}). However, the biomass loss is gradual as sloughing friction velocity increases.

For the three sections, the sloughing test eventually led to the detachment of some proportion of the biomass covering the hemispheres. Indeed, some of the biofilm strongly attached to the artificial cobbles remained after the sloughing test (Table 2), while some of it, composed mostly of filaments, was taken away by the flow. The proportion of detached biomass is inversely proportional to the time-averaged value of friction velocity u_* exerted during biofilm growth (see Table 2). This is in accordance with the results of Waesche et al. (2002); Stoodley et al., 2002 and Möhle et al., 2007, on the effect of growth phase hydrodynamics on the mechanical properties and the resistance to detachment of microbial biofilms. In fact these last studies concluded also that biofilms grown under higher shear were more strongly attached and were cohesively stronger than those grown under lower shears.

4. Conclusion

The impacts of different flow regimes on the dynamics of epilithic biofilm, its structure, algal composition and feedback on the local hydrodynamics have been evidenced by changes in the biomass and algal composition analysis. Actually, the biofilm composition and structures are expressed as different growth forms in relation to hydrodynamic descriptors. Their prevalence and the biofilm thickness is tightly related to the hydrodynamic conditions: *Melosira moniliformis (O.F.Muller) Agardh* was the dominant species in the three sections, while the Indicator Species Analysis (*IndVal*) shows that the indicator taxa were *Fragilaria capucina* var. *mesolepta* in the low-velocity (u_* = 0.010–0.012 m s^{-1}), *Navicula atomus*, *N. capitatoradiata* and *Nitzschia frustulum* in the intermediate-velocity (u_* = 0.023–0.030 m s^{-1}) and *A. pediculus*, *Cymbella proxima*, *Fragilaria capucina* var. *vaucheriae* and *Surirella angusta* in the high-velocity group (u_* = 0.033–0.050 m s^{-1}). An inverse relationship was found between the proportion of detached biomass and the averaged value of friction velocity during biofilm growth. Thus, the differences in biofilm structure and composition, their influence on the flow and their resistance to higher hydrodynamical regimes seem to be a function of the friction velocity u_* on the boundary layer. This result supports the improvement of Labiod et al. (2007) and Graba et al. (2010) in modelling epilithic biomass dynamics with the equation from Uehlinger et al. (1996). This, by substituting the flow discharge with friction velocity or roughness Reynolds number k^+, as an external physical variable forcing the chronic detachment process. This result also sheds new light on the role of local

hydrodynamics in the catastrophic detachment process associated with floods. Firstly, it suggests improving the term describing this process in the same way by considering local hydrodynamic rather than flow and mean velocity, as external physical variables for forcing the detachment process, in epilithic biofilms biomass dynamics models (e.g. Uehlinger et al., 1996; Saravia et al., 1998; Asaeda and Hong Son, 2000, 2001; Flipo et al., 2004; Boulêtreau et al., 2006, 2008). Secondly, the detached biofilm biomass driven by a strong hydraulic perturbation is almost entirely associated with the biofilm filaments, and the results presented here support a separate description of the biomass of these filaments in biofilm dynamics modelling.

Acknowledgements

This work has been supported by the national research project « EC2CO Ecosphère Continentale et Côtière» as part of a project entitled «Couplage et flux entre un biofilm de rivière et un écoulement turbulent : expérimentations en conditions naturelles contrôlées et modélisation numérique dans l'écosystème de la Garonne Moyenne». We wish to thank S. Font, Y. Peltier, C. Pen and D. Baque for technical support, data acquisition and analysis.

REFERENCES

Asaeda, T., Hong Son, D., 2000. Spatial structure and populations of a periphyton community: a model and verification. Ecological Modelling 133, 195–207.

Asaeda, T., Hong Son, D., 2001. A model of the development of a periphyton community resource and flow dynamics. Ecological Modelling 137, 61–75.

Battin, T.J., Kaplan, L.A., Newbold, J.D., Cheng, X., Hansen, C., 2003. Effects of current velocity on the nascent architecture of stream microbial biofilms. Applied and Environmental Microbiology 69, 5443–5452.

Bendat, J.S., Piersol, A., 1971. Random Data: Analysis and Measurement Procedures, second ed. John Wiley & sons Inc., New York (revised and expanded).

Besemer, K., Singer, G., Hodl, I., Limberger, R., Chlup, A.K., Hochedlinger, G., Hodl, I., Baranyi, C., Battin, T.J., 2007. Biophysical controls on community succession in stream biofilms. Applied and Environmental Microbiology 73 (15), 4966–4974. http://dx.doi.org/10.1128/AEM.00588-07.

Besemer, K., Singer, G., Hodl, I., Battin, T.J., 2009a. Bacterial community composition of stream biofilms in spatially variable-flow environments. Applied and Environmental Microbiology 75, 7189–7195.

Besemer, K., Hodl, I., Singer, G., Battin, T.J., 2009b. Architectural differentiation reflects bacterial community structure in stream biofilms. Multidisciplinary Journal of Microbial Ecology 3 (11), 1318–1324.

Biggs, B.J.F., Hickey, C.W., 1994. Periphyton responses to a hydraulic gradient in a regulated river in New Zealand. Freshwater Biology 32 (1), 49–59.

Biggs, B.J.F., Nikora, V.I., Snelder, T.H., 2005. Linking scales of flow variability to lotic ecosystem structure and function. River Research and Applications 21, 283–298.

Blum, J.L., 1957. The ecology of river algae. The Botanical Review 22 (5), 291–341. http://dx.doi.org/10.1007/BF02872474.

Boulêtreau, S., Garabetian, F., Sauvage, S., Sánchez-Pérez, J.M., 2006. Assessing the importance of self-generated detachment process in river biofilm models. Freshwater Biology 51 (5), 901–912. http://dx.doi.org/10.1111/j.1365-2427.2006.01541.x.

Boulêtreau, S., Izagirre, O., Garabetian, F., Sauvage, S., Elosegi, A., Sánchez-Pérez, J.M., 2008. Identification of a minimal adequate model to describe the biomass dynamics of river epilithon. River Research and Applications 24 (1), 36–53. http://dx.doi.org/10.1002/rra.1046.

Boulêtreau, S., Sellali, M., Elosegi, A., Nicaise, Y., Bercovitz, Y., Moulin, F., Eiff, O., Sauvage, S., Sánchez-Pérez, J.M., Garabetian, F., 2010. Temporal dynamics of river biofilm in constant flows: a case study in a riverside laboratory flume. International Review of Hydrobiology 95 (2), 156–170. http://dx.doi.org/10.1002/iroh.200911203.

Cardinale, B.J., 2011. Biodiversity improves water quality through niche partitioning. Nature 472 (3741), 86–89. http://dx.doi.org/10.1038/nature09904.

Castro, I.P., Cheng, H., Reynolds, R., 2006. Turbulence over urban-type roughness: deductions from wind-tunnel measurements. Boundary-layer Meteorology Vol. 118 (1), 109–131.

Clarke, K.R., Gorley, R.N., 2005. In: Plymouth Routines in Multivariate Ecological Research (PRIMER). PRIMER-E Ltd, Plymouth.

Coceal, O., Thomas, T., Castro, I., Belcher, S., 2006. Mean flow and turbulence statistics over groups of urban-like cubical obstacles. Bound-layer Meteor 121, 491–519.

Davis, J.A., Barmuta, L.A., 1989. An ecologically useful classification of mean and near-bed flows in streams and rivers. Freshwater Biology 21, 271–282.

Dufrène, M., Legendre, P., 1997. Species assemblages and indicator species: the need for a flexible asymmetrical approach. Ecological Monographs 67, 345–366.

Fincham, A.M., Delerce, G., 2000. Advanced optimization of correlation imaging velocimetry algorithms. Experiments in Fluids 39 (suppl), S13–S22.

Fincham, A.M., Spedding, G.R., 1997. Low cost, high resolution DPIV measurements of turbulent fluid flow. Experiments in Fluids 23, 449–462.

Flipo, N., Even, S., Poulin, M., Tusseau-Vuillemin, M.H., Ameziane, T., Dauta, A., 2004. Biogeochemical Modelling at the River Scale: Plankton and Periphyton Dynamics.

Fuller, R.L., Roelofs, J.L., Frys, T.J., 1986. The importance of algae to stream invertebrates. Journal of the North American Benthological Society 5, 290–296.

Ghosh, M., Gaur, J.P., 1998. Current velocity and the establishment of stream algal periphyton communities. Aquatic Botany 60 (1), 1–10.

Godillot, R., Ameziane, T., Caussade, B., Capblanc, J., 2001. Interplay between turbulence and periphyton in rough open-channel flow. Journal of Hydraulic Research 39 (3), 227–239.

Graba, M., Moulin, F.Y., Boulêtreau, S., Garabétian, F., Kettab, A., Eiff, O., Sanchez-Pérez, J.M., Sauvage, S., 2010. Effect of near-bed turbulence on chronic detachment of epilithic biofilm in artificial rough, open channel flow: experimental and modeling approaches. Water Resources Research 46, W11531. http://dx.doi.org/10.1029/2009WR008679.

Hondzo, M., Wang, H., 2002. Effects of turbulence on growth and metabolism of periphyton in a laboratory flume. Water Resources Research 38 (12), 1277. http://dx.doi.org/10.1029/2002WR001409.

Horner, R.R., Welch, E.B., 1981. Stream periphyton development in relation to current velocity and nutrients. Canadian Journal of Fisheries and Aquatic Sciences 38 (4), 449–457.

Horner, R.R., Welch, E.B., Veenstra, R.B., 1983. Development of nuisance periphytic algae in laboratory streams in relation to enrichment and velocity. In: Wetzel, R.G. (Ed.), Periphyton of Freshwater Ecosystems. W. Junk Publishers, The Hague, pp. 121–164.

Jowett, I.G., Richardson, J., Biggs, B.J.F., Hickey, C.W., Quinn, J.M., 1991. Microhabitat preferences of benthic invertebrates and the development of generalized *Deleatidium* spp. Habitat suitability curves, applied to four New Zealand rivers. New Zealand Journal of Marine and Freshwater Research 25, 187–199.

Labiod, C., Godillot, R., Caussade, B., 2007. The relationship between stream periphyton dynamics and near-bed turbulence in rough open-channel flow. Ecological Modelling 209 (2–4), 78–96. http://dx.doi.org/10.1016/j.ecolmodel.2007.06.011.

Leflaive, J., Boulêtreau, S., Buffan-Dubau, E., Ten-Hage1, L., 2008. Temporal patterns in epilithic biofilm-relation with a putative allelopathic activity. Archiv für Hydrobiologie 173 (2), 121–134. http://dx.doi.org/10.1127/1863-9135/2008/0173-0121.

Lock, M.A., John, P., 1979. The effect of flow patterns on uptake of phosphorus on river periphyton. Limnology and Oceanography 24, 376–383.

Lock, M.A., Wallace, R.R., Costerton, J.W., Ventullo, R.M., Charlton, S.E., 1984. River epilithon: towards a structural-functional model. Oikos 42, 10–22.

Martínez De Fabricius, A.L., Maidana, N., Gómez, N., Sabater, S., 2003. Distribution patterns of benthic diatoms in a Pampean river exposed to seasonal floods: the Cuarto River (Argentina). Biodiversity and Conservation 12 (12), 2443–2454. http://dx.doi.org/10.1023/A:1025857715437.

Mayer, M.S., Likens, G.E., 1987. The importance of algae in a shaded head water stream as a food of an abundant caddisfly (Trichoptera). Journal of the North American Benthological Society 6, 262–269.

McCune, B., Mefford, M.J., 1999. In: PC-ORD, Multivariate Analyses of Ecological Data. MjM Software Design, Glenenden Beach.

McIntire, C., 1973. Periphyton dynamics in laboratory streams: a simulation model and its implications. Ecological Monographs 34 (3), 399–420.

Minshall, G.W., 1978. Autotrophy in stream ecosystems. BioScience 28, 767–771.

Möhle, R.B., Langemann, T., Haesner, M., Augustin, W., Scholl, S., Neu, T.R., Hempel, D.C., Horn, H., 2007. Structure and shear strength of microbial biofilms as determined with confocal laser scanning microscopy and fluid dynamic gauging using a novel rotating disc biofilm reactor. Biotechnology and Bioengineering 98 (4), 747–755. http://dx.doi.org/10.1002/bit.21448.

Momo, F., 1995. A new model for periphyton growth in running waters. Hydrobiologia 299 (3), 215–218.

Moulin, F.Y., Peltier, Y., Bercovitz, Y., Eiff, O., Beer, A., Pen, C., Boulêtreau, S., Garabetian, F., Sellali, M., Sanchez-Perez, J., Sauvage, S., Baque, D., 2008. Experimental study of the interaction between a turbulent flow and a river biofilm growing on macrorugosities. In: Advances in Hydro-science and Engineering, vol. VIII. ICHE-IAHR, Nagoya, Japan, pp. 1887–1896.

Nezu, I., Nakagawa, H., 1993. Turbulence in Open-channel Flows. Balkema, Rotterdam, The Netherlands.

Nielsen, T.S., Funk, W.H., Gibbons, H.L., Duffner, R.M., 1984. A comparison of periphyton growth on artificial and natural substrates in the upper Spokane River. Northwest Science 58, 243–248.

Nikora, V., Goring, D., Biggs, B., 1997. On stream periphyton-turbulence interactions. The New Zealand Journal of Marine and Freshwater Research 31 (4), 435–448.

Nikora, V., Goring, D., Biggs, B., 1998. A simple model of stream periphyton-flow interactions. Oikos 81 (3), 607–611.

Nikora, V., Goring, D., Biggs, B., 2002. Some observations of the effects of micro-organisms growing on the bed of an open channel on the turbulence properties. The Journal of Fluid Mechanics 450, 317–341.

Nikora, V., McEwan, I., McLean, S., Coleman, S., Pokrajac, D., Walters, R., 2007a. Double averaging concept for rough-bed open-channel and overland flows: theoretical background. Journal of Hydraulic Engineering 133 (8), 873–883. http://dx.doi.org/10.1061/(ASCE)0733-9429(2007)133:8(873).

Nikora, V., McLean, S., Coleman, S., Pokrajac, D., McEwan, I., Campbell, L., Aberle, J., Clunie, D., Kol, K., 2007b. Double-averaging concept for rough-bed open-channel and overland flows: applications background. Journal of Hydraulic Engineering 133 (8), 884–895. http://dx.doi.org/10.1061/(ASCE)0733-9429(2007)133:8(884).

Power, M.E., Stewart, A.J., 1987. Disturbance and recovery of an algal assemblage following flooding in an Oklahoma stream. American Midland Naturalist 117, 333–345.

Reiter, M.A., 1986. Interactions between the hydrodynamics of flowing water and development of a benthic algal community. Journal of Freshwater Ecology 3 (4), 511–517.

Reiter, M.A., 1989a. Development of benthic algal assemblages subjected to differing near substrate hydrodynamic regimes. Canadian Journal of Fisheries and Aquatic Sciences 46, 1375–1382.

Reiter, M.A., 1989b. The effect of a developing algal assemblage on the hydrodynamics near substrates of different size. Archiv für Hydrobiologie 115 (2), 221–244.

Riber, H.H., Wetzel, R.G., 1987. Boundary layer and internal diffusion effects on phosphorus fluxes in lake periphyton. Limnology and Oceanography 32, 1181–1194.

Saravia, L., Momo, F., Boffi Lissin, L.D., 1998. Modeling periphyton dynamics in running water. Ecological Modelling 114 (1), 35–47.

Seath, R.G., Hambrook, J.A., 1988. Mechanical adaptations to flow in freshwater red algae. Journal of Phycology 24, 107–111.

Silvester, N.R., Sleigh, M.A., 1985. The forces on microorganisms at surfaces in flowing water. Freshwater Biology 15, 433–448.

Singer, G., Besemer, K., Schmitt-Kopplin, P., Hodl, I., Battin, T.J., 2010. Physical heterogeneity increases biofilm resource use and its molecular diversity in stream mesocosms. PLoS ONE 5 (4), e9988.

Stoodley, Paul, Boyle, John, D., Lappin-Scott, Hilary, M., 2000. Influence of flow on the structure of bacterial biofilms. In: Bell, Colin R., Brylinsky, M., Johnson-Green, Perry Clark (Eds.), Microbial Biosystems: New Frontiers: Proceedings of the 8th International Symposium on Microbial Ecology. Atlantic Canada Society for Microbial Ecology, pp. 263–269.

Stoodley, P., Cargo, R., Rupp, C.J., Wilson, S., Klapper, I., 2002. Biofilm material properties as related to shear-induced deformation and detachment phenomena. Journal of Industrial Microbiology and Biotechnology 29, 361–367.

Tornés, E., Sabater, S., 2010. Variable discharge alters habitat suitability for benthic algae and cyanobacteria in a forested Mediterranean stream. Marine and Freshwater Research 61, 441–450.

Uehlinger, U., Buhrer, H., Reichert, P., 1996. Periphyton dynamics in a flood-prone pre-alpine river: evaluation of significant processes by modelling. Freshwater Biology 36, 249–263.

Uehlinger, U., Kawecka, B., Robinson, C.T., 2003. Effects of experimental floods on periphyton and stream metabolism below a high dam in the Swiss Alps (River Spöl). Aquatic Sciences 199–209. http://dx.doi.org/10.1007/s00027-003-0664-7.

Waesche, S., Horn, H., Hempel, D.C., 2002. Influence of growth conditions on biofilm development and mass transfer at the bulk/biofilm interface. Water Research 36 (19), 4775–4784.

Wehr, J.D., Sheath, R.G., 2003. In: Wehr, John D., Sheath, Robert G. (Eds.), Freshwater Algae of North America. Academic Press, ISBN 978-0-12-741550-5.

Winterbourn, M.J., 1990. Interactions among nutrients, algae and invertebrates in New Zealand mountain stream. Freshwater Biology 23, 463–474.

Whitford, L.J., Shumacher, G.J., 1961. Effects of current on mineral uptake and respiration by a freshwater alga. Limnology and Oceanography 6, 423–425.

Young, W.J., 1992. Clarification of the criteria used to identify near-bed flow regimes. Freshwater Biology 28, 383–391.